https://doi.org/10.15407/ujpe66.2.151

L.A. BULAVIN,[1] M.A. ALIEKSANDROV,[1] A.I. MISIURA,[1] T.M. PINCHUK-RUGAL',[1] A.P. ONANKO,[1] YU.YE. GRABOWSKIY,[1] O.P. DMYTRENKO,[1] M.P. KULISH,[1] O.L. PAVLENKO,[1] T.O. BUSKO,[1] I.P. PUNDYK,[1] A.I. LESIUK,[1] V.V. STRELCHUK[2]

[1] Taras Shevchenko National University of Kyiv
(64/13, Volodymyrs'ka Str., Kyiv 01601, Ukraine; e-mail: mrmarafon@gmail.com)
[2] V.E. Lashkaryov Institute of Semiconductor Physics, Nat. Acad. of Sci. of Ukraine
(41, Nauky Ave., Kyiv 03028, Ukraine)

MECHANISMS OF STRUCTURAL TRANSFORMATIONS IN POLYETHYLENE NANOCOMPOSITES WITH MULTI-WALLED CARBON NANOTUBES

The dynamic elastic Young, E', and shear, G', moduli in low-density polyethylene nanocomposites with multi-walled carbon nanotubes (MWCNTs) have been studied. It is shown that those parameters are nonmonotonic with the increasing nanotube concentration. The orientational structure of macromolecules adsorbed on nanotubes begins to play an important role, as the MWCNT content grows. Its modification gives rise to changes in the vibrational spectra and the electronic structure of composites and, as a result, may improve their mechanical and transport properties.

K e y w o r d s: nanocomposites, dynamic elastic modulus, dynamic shear modulus, physical and mechanical properties.

1. Introduction

The structure and geometry of carbon nanotubes (CNTs) lead to a number of their unique mechanical, sorptional, heat-conducting, and transport properties [1–5], which allows them to be considered among the most perfect fillers for polymer nanocomposites. The application of CNTs in polymer matrices makes it possible to reach ultra-low values of the electrical conductivity percolation threshold [6–8] and to substantially improve the mechanical properties of the matrices [9]. This improvement takes place because of the interaction between the polymer macrochains and nanotubes, which results in the formation of immobilized layers on CNTs [10–12].

At the same time, the indicated layers containing oriented macromolecules can be characterized by various chain conformations and correspond to different structures [14, 15]. The aim of this work was to determine both the specific features in the intramolecular structure of low-density polyethylene nanocomposites with multi-walled carbon nanotubes and the mechanisms responsible for the concentration dependences of the dynamic mechanical properties.

2. Experimental Technique

In this work, low-density polyethylene (LDPE, Ukraine) with a molecular weight of 80,000 and a melting point of 108–110 °C was used. Car bon nanotubes were synthesized by the low-temperature cat-

alytic conversion of carbon monoxide in the presence of hydrogen. Iron oxides were used as catalysts. The role of catalyst was played by a fine powder of Fe particles used to fill the reactor. The temperature in the reactor was 1,000–1,300 K. The nanotubes were purified from impurities by etching them in the solution $NH_4F : HF : H_2O : HCl$. The diameter of carbon nanotubes was $D = 100$ nm, and the length $l = 1.2$ μm.

Polyethylene composites with multi-walled carbon nanotubes (MWCNTs) were fabricated using the hot-pressing method. The CNT and LDPE components were weighed on a balance with an accuracy of 0.0001 g. Afterward, they were mixed for 5 min in an ultrasonic bath in glasses with warm (60 °C) water and a small amount of alcohol. Then those glasses were left on a table for several days until the alcohol completely evaporated. The dried mixture was mixed again, but manually, in order to detach it from the glass wall, so that it could be poured into a press mold. After pouring the mixture into the mold, it was heated to a temperature of 125–130 °C, which was measured using a thermocouple arranged in a special hole in the mold. Then the mold was placed into a press, subjected to a load of 100 bar (10 MPa), and finally cooled down using a fan. The load and the air flow were kept constant during the process of mold cooling to room temperature (for 30 min). The obtained LDPE-MWCNT composites had the form of disks 30 mm in diameter and 1.5 mm in thickness.

The concentration of nanotubes in the polymer matrix was 0–0.030 vol. frac. The volume concentration of nanotubes in the polymer matrix, $\varphi_{\rm f}$, was calculated according to the formula:

$$\varphi_{\rm f} = \frac{C_{\rm f}\, d_{\rm p}}{C_{\rm f}\, d_{\rm p} + C_{\rm p}\, d_{\rm f}}, \tag{1}$$

where $C_{\rm f}$ is the filler mass fraction, $C_{\rm p}$ the polymer mass fraction, $d_{\rm f}$ the filler density, and $d_{\rm p}$ the polymer density.

The mechanical properties of LDPE-MWCNT nanocomposites were studied with the help of a computerized ultrasonic velocity meter KERN-4 (Ukraine). The dynamic elastic Young modulus was determined using the formula

$$E' = \rho V_{\rm l}^2, \tag{2}$$

where ρ is the specimen density, and $V_{\rm l}$ the velocity of quasilongitudinal ultrasonic elastic waves. The dynamic shear modulus was determined according to the formula

$$G' = \rho V_{\rm tr}^2, \tag{3}$$

where $V_{\rm tr}$ is the velocity of quasitransverse ultrasonic elastic waves. The error of velocity measurements was 1%.

The Raman spectra were measured in the refection geometry and at room temperature on a Horiba Jobin Yvon T64000 triple spectrometer (Japan) equipped with a cooled CCD detector. The spectra were excited by an Ar–Kr ion laser line with the wavelength $\lambda_L = 488$ nm. To excite the photoluminescence (PL) spectra, the lines of a continuous He–Cd laser with the wavelength $\lambda_L = 325$ nm and an Ar–Kr ion laser with the wavelength $\lambda_L = 488$ nm were used. The spectral resolution of the device was 0.015 $\rm cm^{-1}$. The Raman and PL spectra were resolved into components with the help of the PeakFit v4.11 software (the Gauss+Lor contour, the number of iterations $r = 0.998$).

3. Results and Their Discussion

The concentration dependences of the dynamic elastic Young modulus E' and the dynamic shear modulus G' are shown in Fig. 1.

The behavior of the dynamic elastic Young modulus E' is non-monotonic with the increasing nanotube concentration (Fig. 1, *a*). As the MWCNT content becomes higher, the orientational structure of macromolecules adsorbed on the nanotubes begins to play an important role. The role of indicated structured layers also increases at that. One can see that the dynamic modulus E' first increases drastically at low concentrations. Afterward, the reached value is maintained with a tendency to a slight growth owing to the formation of an oriented structure in the considered layers [9, 10].

Such a behavior is not exactly reproduced for the shear modulus G' (Fig. 1, *b*). The orientational structure of macromolecules in the polymer layers between neighbor nanotubes plays an important role in maintaining the enhanced value of G' in a wide concentration interval. Since the appearance of a polymer layer with a specific structure is a result of the interaction between the phases, its presence should be accompanied by a reconstruction of vibrational and photoluminescent spectra [16–18].

In Fig. 2, the Raman spectrum obtained for LDPE at the excitation wavelength $\lambda_{\text{exc}} = 488$ nm is shown. One can see that, in a frequency interval of 1000–3000 cm^{-1}, the spectrum can be divided into low- and high-frequency sections. The observed bands correspond to the vibrational modes of C–C and C–H bonds in trans-chains and macromolecules in the crystalline and amorphous polymer phases. The frequencies of those bands are indicated in Fig. 3.

The 1065-cm^{-1} band corresponds to asymmetric stretching vibrations of the C–C bond in the molecular backbone in the trans-chains with the symmetry type $B_{2g} + B_{3g}$ [v_{as} (C–C)]. The low-intensity band at 1082 cm^{-1} corresponds to the stretching vibrations of the C–C bond in the amorphous phase [v_{as} (C–C)], and the band at 1131 cm^{-1} is associated with the symmetric stretching vibrations in the trans-chains with the symmetry type $A_g + B_{1g}$ [v_s (C–C)]. The next intensive band at 1298 cm^{-1} corresponds to torsional vibrations in the crystalline phase with the symmetry type $B_{2g} + B_{3g}$ [v_t (C–C)]. The next three bands at 1421, 1441, and 1462 cm^{-1}, unlike the previous bands associated with stretching vibrations or torsional vibrations of the C–C bond in the macromolecular backbone, are connected with bending (deformation) vibrations and vibrations of CH_2 groups.

In particular, the band at 1421 cm^{-1} is associated with deformation vibrations $\delta(CH_2)$ and pendulum vibrations $\omega(CH_2)$ in the crystalline phase characterized by an orthorhombic structure with the symmetry type A_g. The band at 1441 cm^{-1} corresponds to deformation vibrations $\delta(CH_2)$ in the amorphous phase of polyethylene trans-chains with the symmetry type $A_g + B_{1g}$. Symmetric stretching vibrations $v_s(CH_2)$ result in the appearance of a band at about 2854 cm^{-1} with the symmetry type $A_g + B_{1g}$, and asymmetric stretching vibrations $v_{\text{as}}(CH_2)$ in the appearance of a band at 2885 cm^{-1}. The other bands are classified as a manifestation of the Fermi resonance between fundamental vibrations (2725 cm^{-1}) and are related to the second-order spectral bands (at 2902 and 2917 cm^{-1}) or to symmetric and asymmetric vibrations of methyl groups (CH_2), i.e. $v_s(CH_3)$ and $v_{\text{as}}(CH_3)$, respectively [19–21].

The doping of polyethylene with nanotubes to 0.001 vol. frac. resulted in the band shift. For instance, the band at 1065 cm^{-1} shifted to 1064 cm^{-1}, and the band at 1082 cm^{-1} to 1086 cm^{-1}. The band

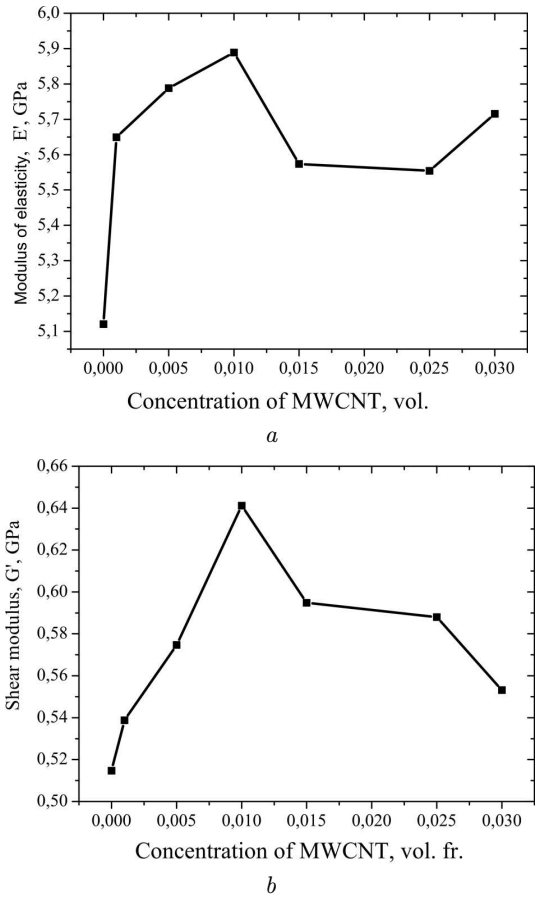

Fig. 1. Concentration dependences of the dynamic elastic Young E' (a) and shear G' (b) moduli for LDPE-MWCNT nanocomposites. The frequency is 1 MHz for E' and 0.7 MHz for G'

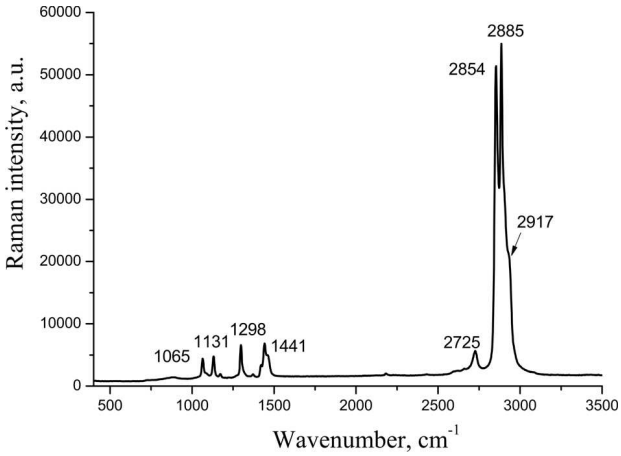

Fig. 2. Raman spectrum of LDPE. $\lambda_{\text{exc}} = 488$ nm and $T = 298$ K

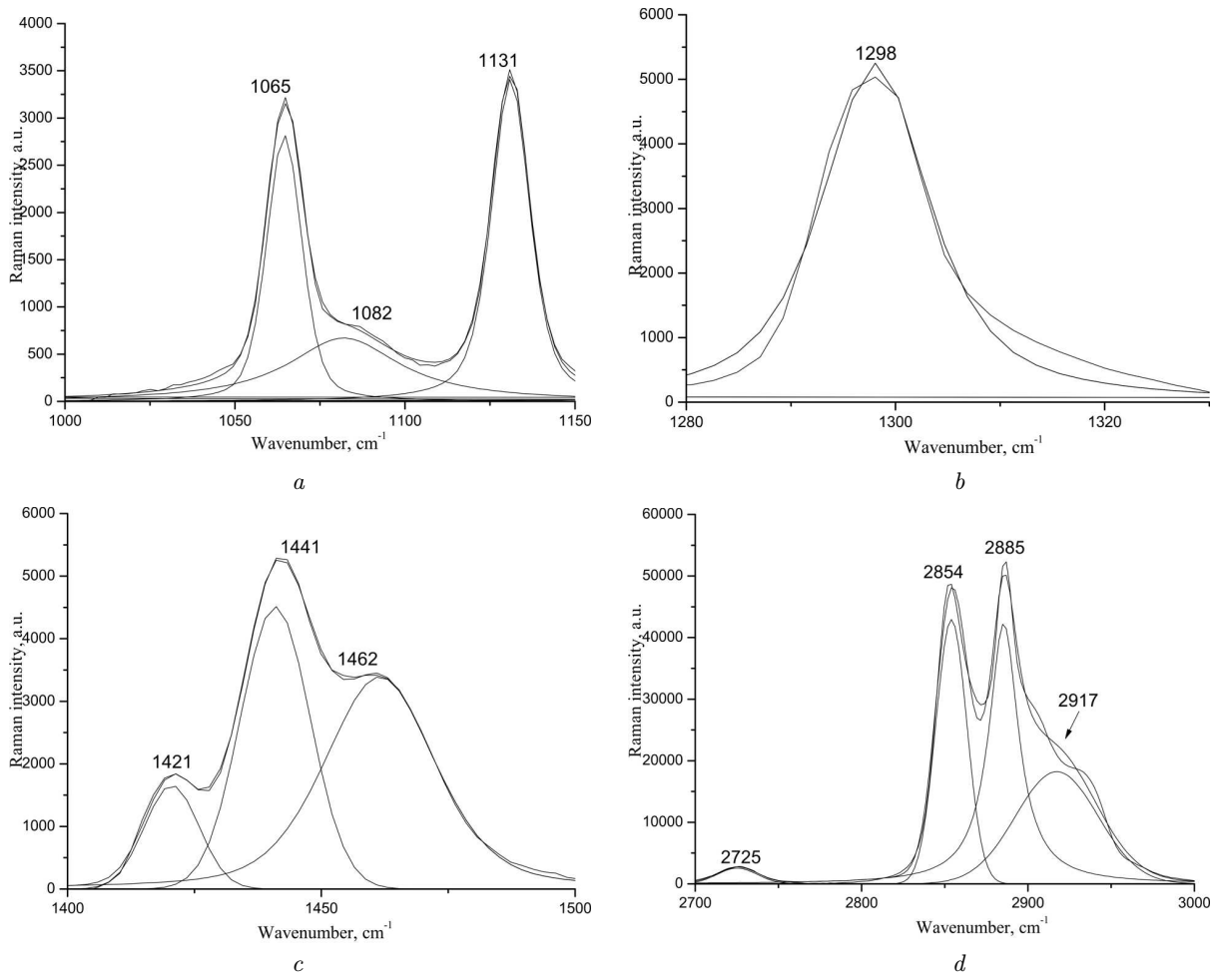

Fig. 3. Raman spectra of LDPE in the spectral intervals of 1000–1150 (a), 1280–1330 (b), 1400–1500 (c), and 2700–3000 cm^{-1} (d) and their resolution into components. $\lambda_{exc} = 488$ nm and $T = 298$ K

of vibrational mode $\delta(CH_2)$ also shifted to lower frequencies: from 1462 to 1455 cm^{-1}. Analogously, the band at 2885 cm^{-1} shifted to 2886 cm^{-1} (see Fig. 4).

A similar scenario of the intensity redistribution in the Raman spectrum is observed at a nanotube concentration of 0.005 vol. frac. A substantial reconstruction in the Raman spectrum for the LDPE-MWCNT nanocomposite occurs at a nanotube concentration of 0.03 vol. frac. In particular, there appear an intensive band at 860 cm^{-1} and less intensive bands at 130 and 104 cm^{-1}, which correspond to the pendulum vibrations of the methylene group CH_2. In addition, there emerge low-intensity bands in the interval of 1500–1600 cm^{-1}, which correspond to the presence of MWCNTs.

Hence, if the concentration of nanotubes is low, they favor an enhancement of the crystallization degree and the formation of a macrochain trans-conformation. An increase of the MWCNT concentration, on the contrary, leads to the structure amorphization and the simultaneous growth of the fraction of oriented macromolecules in the trans-conformation. Hence, we may assert that the formation of oriented layers with the trans-conformation of macromolecules, which occurs at higher nanotube concentrations as a result of interaction between the phases at the filler surface, is the main mechanism responsible for the growth of the dynamic elastic and shear moduli.

Polyethylene, like the overwhelming majority of polymers, does not absorb light in the visible spectral

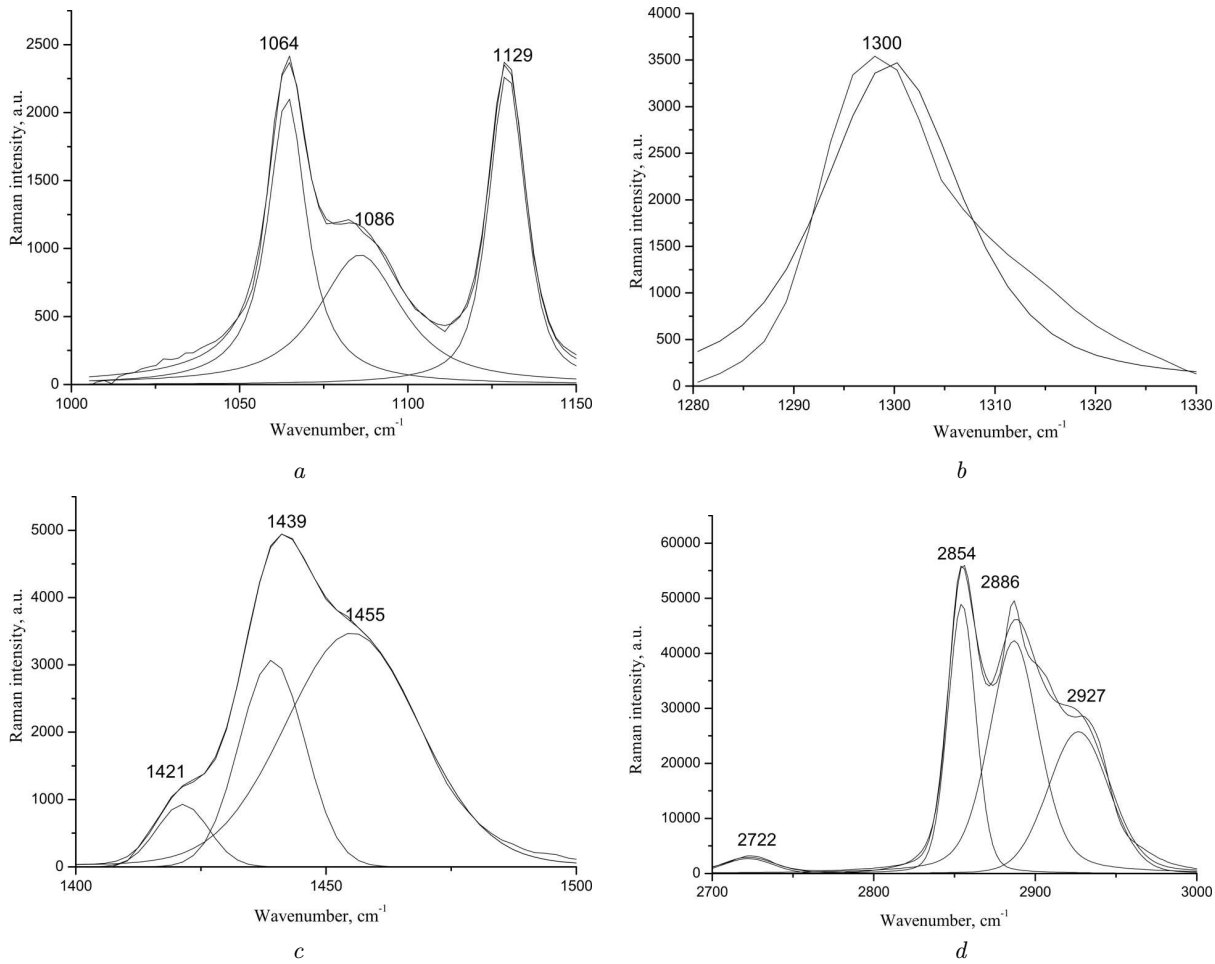

Fig. 4. Raman spectra of LDPE-MWCNT nanocomposite with a nanotube concentration of 0.001 vol. frac. in the spectral intervals of 1000–1150 (*a*), 1280–1330 (*b*), 1400–1500 (*c*), and 2700–3000 cm^{-1} (*d*) and their resolution into components. $\lambda_{\text{exc}} =$ $= 488$ nm and $T = 298$ K

interval. The absorption, fluorescence, and phosphorescence phenomena become possible only owing to the appearance of defect electronic levels localized in the energy gap. Such defects may include diene and polyene structures [22–25]. They can arise as a result of the interaction between the macromolecules and the fillers, first of all in the considered immobilized layers. The mechanochemical action of the filler leads to a variation in the number of vinylene, vinyl, and terminal double bonds. In addition, polyene structures, which are entities with delocalized electrons, should facilitate the charge transfer in the polymer matrix [26–29]. As a result, the formation of polyene structures may improve the tunnel transitions of electrons in the polymer matrix.

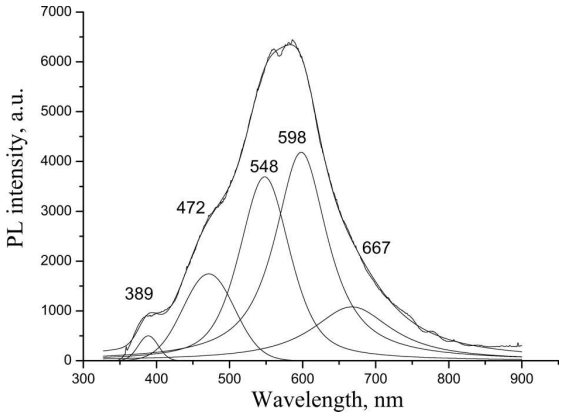

Fig. 5. PL spectrum of LDPE and its resolution into components. $\lambda_{\text{exc}} = 325$ nm and $T = 298$ K

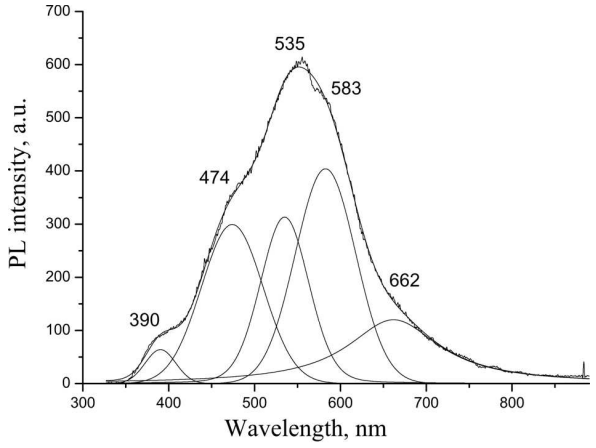

a

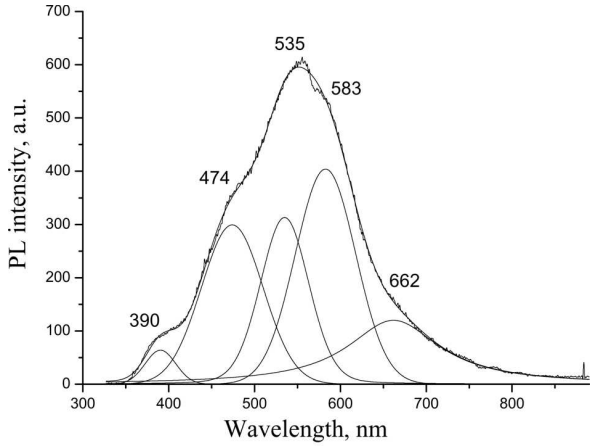

b

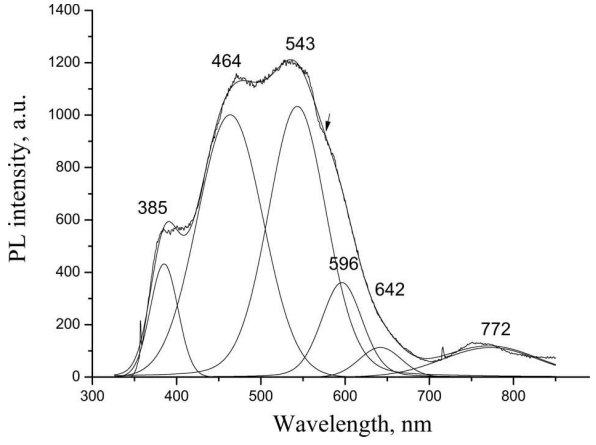

c

Fig. 6. PL spectra of LDPE-MWCNT nanocomposites with nanotube concentrations of 0.001 (*a*), 0.005 (*b*), and 0.03 vol. frac. (*c*) and their resolution into components

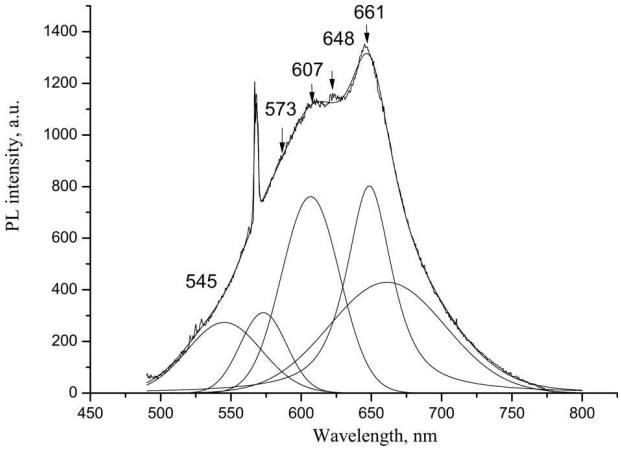

Fig. 7. PL spectrum of LDPE-MWCNT nanocomposite with a nanotube concentration of 0.03 vol. frac. $\lambda_{exc} = 488$ nm

Figure 5 demonstrates the fluorescence spectrum of LDPE at its excitation at the wavelength $\lambda_{exc} = 325$ nm. It is evident that the PL spectrum of LDPE in the initial state consists of several components, which are associated with the recombination of broken C–C bonds (at 389 nm), oxides with carbonyl C=O groups (at 472 nm), and polyenes of different lengths (at 548, 598, and 667 nm) belonging to the types $–CH_2–CH=CH_2–CH_2–CH–$ and $–CH=CH–CH=CH_2$ [30]. After the doping of polyethylene with nanotubes, the PL spectrum becomes substantially reconstructed (Fig. 6).

The reconstruction begins already at a nanotube concentration of 0.001 vol. frac., but the corresponding peak shifts are insignificant. At higher concentrations (at about 0.005 vol. frac. and, especially, at 0.03 vol. frac.), the PL spectrum becomes considerably shifted toward the short-wavelength region, which testifies to a reduction of the polyene chain length. Furthermore, the PL intensity becomes substantially lower, which may be a result of either its quenching by nanotubes or a reduction in the polyene concentration.

The reconstructions in the PL spectrum become larger at the wavelength $\lambda_{exc} = 488$ nm (see Fig. 7). At this excitation wavelength, the PL spectrum only testifies to the presence of polyene structures with various lengths. Therefore, it is evident that the fillers substantially modify the defect structure of the adsorbed polymer layers. Hence, the mechanical and chemical influences of nanotubes lead to the recon-

struction of the polymer matrix structure, which can strongly affect the contact layer between the nanotubes and, in such a way, modify the mechanical and transport properties of nanocomposites.

4. Conclusions

The concentration behavior of the dynamic elastic and shear moduli in LDPE-MWCNT nanocomposites testifies to the orientational structuring of macromolecules adsorbed on nanotubes. The change in the nanotube concentration gives rise to modifications in the Raman spectra associated with the changes in the orientational structure and conformation of macromolecules that are immobilized on the nanotube surface at low filler contents. Besides structural changes, a reconstruction of defects associated with the emergence of carbonyl groups C=O and polyenes with various lengths also takes place. With the growth of the nanotube concentration, the polyene structures transform toward the reduction of their size. As a result, the energy states become reconstructed, and the photoluminescence spectra change.

1. A.V. Eletskii. Carbon nanotubes. *Usp. Fiz. Nauk* **167**, 945 (1997) (in Russian).
2. A.V. Eletskii. Carbon nanotubes and their emission properties. *Usp. Fiz. Nauk* **172**, 401 (2002) (in Russian).
3. A.V. Eletskii. Sorption properties of carbon nanostructures. *Usp. Fiz. Nauk* **174**, 1191 (2004) (in Russian).
4. A.V. Eletskii. Transport properties of carbon nanotubes. *Usp. Fiz. Nauk* **179**, 225 (2009) (in Russian).
5. A.V. Eletskii. Carbon nanotube-based electron field emitters. *Usp. Fiz. Nauk* **180**, 897 (2010) (in Russian).
6. M.O. Lisunova *et al.* Percolation behaviour of ultrahigh molecular weight polyethylene/multi-walled carbon nanotubes composites. *Eur. Polym. J.* **43**, 949 (2007).
7. Ye.P. Mamunya, V.V. Levchenko, Ye.V. Lebedev. Thermomechanical and electrical properties of segregated polymer nanocomposites based on polyvinyl chloride and carbon nanotubes. *Polimer. Zh.* 30, 324 (2008) (in Ukrainian).
8. A.V. Eletskii, A.A. Knizhnik, B.V. Potapkin, J.M. Kenny. Electrical characteristics of carbon-nanotube doped composites. *Usp. Fiz. Nauk* **185**, 225 (2015) (in Russian).
9. A.V. Eletskii. Mechanical properties of carbon nanostructures and related materials. *Usp. Fiz. Nauk* **177**, 223 (2007) (in Russian).
10. Ya.I. Estrin, E.R. Badamshina, A.A. Grischuk *et al.* Properties of nanocomposites based on crosslinked elastomeric polyurethane and ultra-small additives of single-walled carbon nanotubes. *Vysokomol. Soed. A* **54**, 568 (2008) (in Russian).
11. A.L. Svistkov, L.A. Komar, G. Heinrich *et al.* Modeling of the formation process of oriented polymer layers near filler particles in polymer nanocomposites. *Vysokomol. Soed. A* **50**, 903 (2008) (in Russian).
12. B.A. Komarov, E.A. Dzhavadyan, V.I. Irzhak *et al.* Epoxyamine composites with ultra-low concentrations of single-walled carbon nanotubes. *Vysokomol. Soed. A* **53**, 897 (2011) (in Russian).
13. S. A. Gordeyev, G. Yu. Nikolaeva, K.A. Prokhorov. The Raman study of the structure of oriented polyethylenes. *Laser Phys.* **6**, 121 (1996).
14. K.A. Prokhorov, G.Yu. Nikolaeva, S.A. Gordeyev, P.P. Pashinin, Raman scattering in oriented polyethylene: The C-H stretching region. *Laser Phys.* **11**, 86 (2001).
15. T. McNally, P. Potschke, P. Halley *et al.* Polyethylene multiwalled carbon nanotube composites. *Polymer* **46**, 8222 (2005).
16. O.S. Nychyporenko, O.P. Dmytrenko, M.P. Kulish, T.M. Pinchuk-Rugal', Yu.Ye. Grabowskiy, M.A. Zabolotniy, V.A. Strel'chuk, A.S. Nikolenko, Yu.I. Sementsov, Ye.P. Mamunya. Radiation technologies of polymer composites properties modification. In *Nanotechnology in the Security Systems.* Edited by J. Bonča, S. Kruchinin (Springer, 2013), p. 69.
17. O.S. Nychyporenko, O.P. Dmytrenko, M.P. Kulish *et al.* Radiation-induced structure transformation and vibrational spectra of polyethylene. *Nucl. Phys. At. Energy* **16**, 367 (2015).
18. O.S. Nychyporenko, O.P. Dmytrenko, M.P. Kylish *et al.* Radiation-stimulated alteration of electrical conductivity of polyethylene nanocomposites with carbon nanotubes. *Vopr. At. Nauki Tekhn.* 102, 99 (2016) (in Ukrainian).
19. T. Kida, T. Oku, Y. Hiejima *et al.* Deformation mechanism of high-density polyethylene probed by in situ Raman spectroscopy. *Polymer* **58**. 88 (2015).
20. T. Kida, Y. Hiejima, K-H Nitta. Rheo-optical Raman study of microscopic deformation in high-density polyethylene under hot drawing. *Polymer Test.* **44**, 30 (2015).
21. T. Kida, Y. Hiejima, K-H. Nitta. Raman spectroscopic study of high-density polyethylene during tensile deformation. *Int. J. Exper. Spectrosc. Techn.* **1**, 001 (2016).
22. N. Garcia, M. Koyos, G. Teyssedre *et al.* The grafting of luminescent side groups onto poly(vinyl chloride) and the identification of local structural features, *Polym. Degrad. Stabil.* **92**, 2300 (2007).
23. S. Giuffrida, G.G. Condorelli, L.L. Costanzo. In situ synthesis of photoluminescent films of PVC, doped with Ce^{3+} ion. *J. Photochem. Photobiol. A* **195**, 215 (2008).
24. Z. Osawa, H. Kuroda. Differences in polyene formation between polyethylene and polypropylene during photoirradiation. *Polym. Photochem.* **7**, 231 (1986).
25. S. Balbanov, K. Velitchkova, K. Krezhov. Photoluminescence of carbon-implanted ultra-high molecular weight polyethylene composite and its modification by gamma irradiation. *Vacuum* **69**, 107 (2003).

26. H.M. Zidan, A. Tawansi, M. Abu-Elnader. Miscibility, optical and dielectric properties of UV-irradiated poly(vinylacetate)/poly(methylmethacrylate) blends. *Physica B* **339**, 78 (2003).
27. H.M. Zidan. Filling level effect on the physical properties of $MgBr_2$- and $MgCl_2$-filled poly(vinyl acetate) films. *J. Polymer Sci.* **41**, 112 (2003).
28. H.M. Zidan, M. Abu-Elnader. Structural and optical properties of pure PMMA and metal chloride-doped PMMA films. *Physica B* **335**, 308 (2005).
29. H.M. Zidan, A. El-Khodary, I.A. El-Sayed, H.I. El-Bohy. Optical parameters and absorption studies of UV-irradiated azo dye-doped PMMA films, *J. Appl. Polymer Sci.* **117**, 1416 (2010).
30. M.A. Alieksandrov, T.M. Pinchuk-Rugal, O.P. Dmytrenko, M.P. Kulish, V.V. Shlapatska, V.M. Tkach. Radiation-stimulated formation of polyene structures in polyethylene nanocomposites with multi-walled carbon nanotubes. In *Nanocomposites, Nanostructures, and Their Applications. NANO 2018.* Edited by O. Fesenko, L. Yatsenko (Springer, 2019), p. 323.

Received 13.02.20.
Translated from Ukrainian by O.I. Voitenko

Л.А. Булавін, М.А. Александров, А.І. Місюра, Т.М. Пінчук-Ругаль, А.П. Онанко, Ю.Є. Грабовський, О.П. Дмитренко, М.П. Куліш, О.Л. Павленко, Т.О. Буско, І.П. Пундик, А.І. Лесюк, В.В. Стрельчук

МЕХАНІЗМИ ПЕРЕТВОРЕНЬ СТРУКТУРИ В НАНОКОМПОЗИТАХ ПОЛІЕТИЛЕНУ З БАГАТОСТІННИМИ ВУГЛЕЦЕВИМИ НАНОТРУБКАМИ

Досліджено динамічні модулі пружності, зсуву в нанокомпозитах поліетилену низької густини з багатостінними вуглецевими нанотрубками (ПЕНГ-БВНТ). Показано, що поведінка динамічного модуля пружності Юнга E' та модуля зсуву G' при збільшенні концентрації нанотрубок має немонотонний характер. Зі збільшенням вмісту БВНТ важливу роль відіграє орієнтаційна структурованість макромолекул, адсорбованих на нанотрубках. Це супроводжується перебудовою коливних спектрів та електронної структури і, як наслідок, може впливати на покращення фізико-механічних та транспортних властивостей вказаних нанокомпозитів.

Ключові слова: нанокомпозити, динамічні модулі пружності, зсуву, фізико-механічні властивості.